

Received November 7, 2018, accepted November 21, 2018, date of publication December 5, 2018, date of current version December 31, 2018.

Digital Object Identifier 10.1109/ACCESS.2018.2885144

# A Unified Nonsingular Rapid Transfer Alignment Solution for Tactical Weapon Based on Matrix Kalman Filter

XIAO CUI<sup>1</sup>, GONGMIN YAN<sup>1</sup>, QIANGWEN FU<sup>1</sup>, QI ZHOU<sup>2</sup>,  
AND ZHENBO LIU<sup>1,3</sup>, (Student Member, IEEE)

<sup>1</sup>School of Automation, Northwestern Polytechnical University, Xi'an 710129, China

<sup>2</sup>Xi'an Flight Automatic Control Research Institute, Xi'an 710065, China

<sup>3</sup>Department of Geomatics Engineering, University of Calgary, Calgary, AB T2N 1N4, Canada

Corresponding author: Xiao Cui (cuixiao88@163.com)

This work was supported by the Aeronautical Science Fund of China under Grant 20165853041.

**ABSTRACT** The performance of tactical weapons inertial navigation system (INS) greatly depends on the accuracy and rapidity of transfer alignment (TA). The major challenge is the estimation of the attitude of INS rapidly and accurately, under the condition of random initial misalignment angles and launch time constraint in tactical scenarios. The objective of this paper is to derive a unified nonsingular alignment scheme for rapid TA at random initial misalignment angles, which transforms the alignment problem into the estimation of the relative attitude matrix between the master INS and slave INS. Employing the attitude matrix as estimate state, we formulate a unified nonsingular linear dynamics model allowing us to estimate the attitude matrix directly. Furthermore, the attitude matrix estimation algorithm has been extended to work in a state matrix Kalman filter (MKF) framework, which we call MKFTA algorithm. It works without any assumption on the misalignment angles. Finally, Monte Carlo simulations demonstrate that the MKFTA can converge within 10 s and exhibits a better transient and steady-state accuracy than the traditional scheme.

**INDEX TERMS** Transfer alignment, misalignment, attitude matrix, matrix Kalman filter transfer alignment (MKFTA).

## I. INTRODUCTION

Inertial navigation systems have been proven and widely used in military applications for weapon systems to meet essential requirement for the guidance and control, especially with the improvement of small-sized and low-cost INS. As a dead-reckoning method, the initial alignment error is the main contributor to the subsequent navigation error due to the average flight time being tens of seconds for tactical weapons. Therefore, how to achieve accurate, rapid, and robust initial alignment of INS is indispensable to improve the overall performance of tactical weapon systems [1]. For the low-cost INS, the noise threshold of gyros is too high to detect the Earth's rotation rate properly. In this respect, the initial alignment approach for high-end INS is not feasible for low-cost INS. A popular approach is to use an external aiding sensor to provide additional information as reference for transfer alignment. The transfer alignment has been investigated as one of the key technologies of tactical weapon applications for the last 30 years since 1989 [2],

and has given rise to numerous algorithms following two main approaches, namely, the optimization-based approach and the Kalman filter based approach. The first approach is a constrained least-squares, which is often referred to as Wahba's problem. To solve this problem, numerous algorithms are developed, such as the q-method, QUEST, and REQUEST [3], [4], which compute the optimal quaternion as the eigenvector of a symmetric  $4 \times 4$   $K$  matrix with the eigenvalue [5]–[9]. It is, however, difficult to implement in fine alignment, and it just serves as a coarse alignment scheme due to its inability to estimate anything other than the attitude quaternion [8]–[10]. The Kalman filter approach, on the other hand, became a common topic of research, and allows the estimation of parameters other than attitude by designing state space model [11]–[13]. The linear KF was successfully applied to many works for optimal estimation with small misalignment angles assumption [14], [15], but such assumption does not hold in many practical applications. In such cases, various ways were developed in order to meet the increasing

demands of accurate and rapid alignment with large misalignment angles between the M-INS and S-INS. They are second order Extended Kalman Filter (EKF2) [1], [16],  $H_\infty$  filter [17], adaptive incremental Kalman lter (AIKF) [18], unscented Kalman filter (UKF) [19]–[22] and Particle Filter (PF) [23]–[27]. The problems of these approaches are well-known linearization effects and computational load resulting from the nonlinear filters [28]. Furthermore, some works aimed at improving the TA performance by taking into account the aircraft flexure and lever arm effect [29]–[31], while others addressed the matching methods [2], [15], [32]. In the works mentioned hitherto, researches have been mostly devoted to the alignment vector model at large misalignment in terms of the Rodrigues parameters [1], attitude quaternion [10], [19], and rotation vector [21], which have led to the nonlinear model. Although there are six redundant elements in the attitude matrix, it provides the most convenient parameterization of orientation, and has the most attractive feature that the dynamics model of alignment is linear and nonsingular. Considering this advantage, a unified nonsingular model for rapid transfer alignment is derived without making any assumption on the misalignment angles, which is urgently demand for tactical weapon systems.

The classical Kalman filter was developed to operate on plants which are governed by vector differential equations [33]. As a result, the state vector KF is not naturally suited for the state matrix estimation. Therefore, we use a general state matrix Kalman filter (MKF) [34] for this plant, this is, a KF that provides an optimal estimation in the form of matrix. Compared with all previous works mentioned above, the main contribution of this paper resides in establishing a linear nonsingular matrix state-space model, where the matrix state is estimated under the MKF framework. With respect to our previous work [1], two aspects are improved: the attitude matrix becomes the state and can be cast into a linear measurement equation. As a result, the proposed approach is truly unified transfer alignment model suitable for random misalignment angles and has no singularity (the Rodrigues parameters suffer from the singularity associated with the  $\pi$  rotation about the principal [1], [35]), which is a desired property for developing an automatic transfer alignment algorithm. Furthermore, the attitude matrix system equations are linear, which allows a straightforward estimation without computation of the Hessian matrix (as would be the case in [1]). This is the main guideline that we keep in mind when developing the algorithm to get “the best of both worlds.”

The structure of this paper is organized as follows. First, kinematic and actual measurement relations between master and slave INS systems that are located apart from each other are derived. A unified nonsingular model for rapid transfer alignment at random misalignment angles is designed delicately in the next section focusing on the dynamic equation and measurement equation establishment in terms of attitude matrix. A description of state MKF is given in the following section. Then, the performance of the alignment method is demonstrated and analyzed via Monte-Carlo simulations.

Meanwhile, comparison with existing methods and discussion of flexure effect have been presented, which can further highlight the performance of the developed method. Finally, conclusions are drawn in the last section.

## II. KINEMATIC RELATIONSHIP BETWEEN M-INS AND S-INS

In a typical transfer alignment application, it is difficult to obtain accurate knowledge of the relative position and attitude of M-INS and S-INS. Hence, two navigation systems undergo different motion and their measured parameter are different from each other. In this section, we will look at the kinematics relations between M-INS and S-INS.

### A. THEORETICAL RELATIONSHIP OF PHYSICAL MEASUREMENT VECTORS BETWEEN M-INS AND S-INS

Denote by  $m$  the M-INS body frame, by  $s$  the S-INS body frame, and  $i$  the inertially nonrotating frame. The specific forces relation between the M-INS and S-INS in the inertial frame is, known as ([1], [29]).

$$\mathbf{f}_s^i = \mathbf{f}_m^i + \mathbf{C}_m^i [\boldsymbol{\omega}_{im}^m \times (\boldsymbol{\omega}_{im}^m \times \mathbf{r}_{ms}^m) + \dot{\boldsymbol{\omega}}_{im}^m \times \mathbf{r}_{ms}^m + 2(\boldsymbol{\omega}_{im}^m \times \dot{\mathbf{r}}_{ms}^m) + \ddot{\mathbf{r}}_{ms}^m] \quad (1)$$

where  $\mathbf{f}_m^i$  and  $\mathbf{f}_s^i$  are the specific forces measured by accelerometers of M-INS and S-INS defined in the inertial reference frame, respectively.  $\mathbf{C}_m^i$  denotes the transformation matrix form the M-INS body frame to the inertial frame and  $\mathbf{r}_{ms}^m$  is the position vector known as lever arm from the M-INS to the S-INS in the M-INS body frame.  $\boldsymbol{\omega}_{im}^m$  is the angular rate measured by gyroscopes of M-INS in the M-INS body frame.

It is further assumed that the lever arm is rigid, then equation (1) becomes

$$\mathbf{f}_s^i = \mathbf{f}_m^i + \mathbf{C}_m^i [\boldsymbol{\omega}_{im}^m \times (\boldsymbol{\omega}_{im}^m \times \mathbf{r}_{ms}^m) + \dot{\boldsymbol{\omega}}_{im}^m \times \mathbf{r}_{ms}^m] \quad (2)$$

From the above equation, we can see that the specific force of S-INS can be computed from the outputs of M-INS. The second term on the right side of this equation is known as lever arm compensation, which is denoted as  $\mathbf{f}_{mc}^i$ , then equation (2) can be rewritten as

$$\mathbf{f}_s^i = \mathbf{f}_{mc}^i \quad (3)$$

As another inertial measurement of INS, angular rate information between master and slave systems in three directions can be found by using simple vector addition as follows:

$$\boldsymbol{\omega}_{is}^i = \boldsymbol{\omega}_{im}^i + \boldsymbol{\omega}_{ms}^i \quad (4)$$

where  $\boldsymbol{\omega}_{ms}^i$  represent the angular rate of S-INS with respect to M-INS defined in inertial frame of reference.

### B. ACTUAL MEASUREMENT RELATIONSHIP OF SPECIFIC FORCE AND ANGULAR RATE IN INERTIAL FRAME

Before deriving actual measurement relationship of specific force and angular rate in inertial frame, we use the symbol  $i_m$  to denote an auxiliary inertial nonrotating frame, which

is aligned with the M-INS body frame at the start-up of the alignment and inertially “frozen” after the start-up time epoch. Then, the time-varying attitude matrix  $C_m^{i_m}(t)$  in alignment process due to the attitude changes of the M-INS body frame ( $m$ ) relative to the inertial frame ( $i_m$ ) as a function of inertial angular rate, which is measured by gyros. Its rate equation is

$$\dot{C}_m^{i_m}(t) = C_m^{i_m}(t)\omega_{i_m}^m(t), \quad C_m^{i_m}(0) = I_3 \quad (5)$$

where  $\omega_{i_m}^m(t)$  is the angular rate measured by gyroscopes of M-INS in the body frame. For M-INS, the sensor precision is much higher than that of S-INS, which means that error of M-INS will be ignored in rapid transfer alignment period.

Similarly, we see that

$$\dot{\hat{C}}_s^{i_s}(t) = \hat{C}_s^{i_s}(t)\hat{\omega}_{i_s}^s(t), \quad \hat{C}_s^{i_s}(0) = I_3 \quad (6)$$

where the definition of inertial frame  $i_s$  is similar to frame  $i_m$ .

In the equation (6), assuming that the error of  $\hat{C}_s^{i_s}$  just introduced by gyros bias of S-INS, and the computing platform misalignment angles  $\phi_s^{i_s}$  is small. Then we obtain

$$\begin{cases} \hat{C}_s^{i_s} = [I_3 - (\phi_s^{i_s} \times)] C_s^{i_s} \\ \hat{\phi}_s^{i_s} = -\hat{C}_s^{i_s} [(\epsilon^s + w_g^s)] \end{cases} \quad (7)$$

where the  $\epsilon^s, w_g^s$  are gyroscope biases and noise of S-INS, respectively. The  $3 \times 3$  skew symmetric matrix  $(\cdot \times)$  is defined so that the cross-product satisfies  $a \times b = (a \times) b$  for two arbitrary vectors [5].

According to the equation (2), we can compensate lever arm effects for specific force output of the M-INS. The estimation of compensated specific force  $f_{mc}^m$  is denoted as  $\hat{f}_{mc}^m$ , which can be written as

$$\hat{f}_{mc}^m = f_{mc}^m + w_f^m \quad (8)$$

where the  $w_f^m$  is residue term of lever arm effects.

Multiplying both sides by computed attitude matrix  $C_m^{i_m}(t)$  from equation (5), equation (8) can therefore be rewritten as

$$\hat{f}_{mc}^{i_m} = C_m^{i_m} \hat{f}_{mc}^m = f_{mc}^{i_m} + C_m^{i_m} w_f^m \quad (9)$$

In a similar manner we can use specific force  $f_s^s$  output of the S-INS to obtain that projected in inertial frame  $i_s$

$$\hat{f}_s^{i_s} = \hat{C}_s^{i_s} f_s^s = [I_3 - (\phi_s^{i_s} \times)] C_s^{i_s} (f_s^s + \nabla^s + w_a^s) \quad (10)$$

where the  $\nabla^s, w_a^s$  are accelerometers biases and noise of S-INS, respectively. Expanding this equation while neglecting the higher order slim terms gives

$$\hat{f}_s^{i_s} = f_s^{i_s} + \hat{f}_s^{i_s} \times \phi_s^{i_s} + \hat{C}_s^{i_s} \nabla^s + \hat{C}_s^{i_s} w_a^s \quad (11)$$

From equation (9) and (10), we obtain

$$\hat{f}_s^{i_s} - \hat{f}_s^{i_s} \times \phi_s^{i_s} - \hat{C}_s^{i_s} \nabla^s - \hat{C}_s^{i_s} w_a^s = C_m^{i_s} \hat{f}_{mc}^{i_m} - C_m^{i_m} w_f^m \quad (12)$$

where  $C_m^{i_s}$  is a constant matrix, which represents the initial relationship between M-INS and S-INS body frames at the start-up of the alignment.

In a similar manner, we use the angular rate output of M-INS and S-INS to obtain

$$\hat{\omega}_{i_s}^{i_s} - \hat{\omega}_{i_s}^{i_s} \times \phi_s^{i_s} - \hat{C}_s^{i_s} \epsilon^s - \hat{C}_s^{i_s} w_g^s = C_m^{i_s} \omega_{i_m}^{i_m} + \omega_{i_m}^{i_s} \quad (13)$$

where

$$\begin{cases} \hat{\omega}_{i_s}^{i_s} = \hat{C}_s^{i_s} \hat{\omega}_{i_s}^s \\ \omega_{i_m}^{i_m} = C_m^{i_m} \omega_{i_m}^m \\ \omega_{i_m}^{i_s} = \hat{C}_s^{i_s} \omega_{i_m}^s \end{cases} \quad (14)$$

where  $\omega_{i_m}^s$  is the flexible angle rate, which is modeled as a second order Markov process [1], [10]:

$$\begin{cases} \dot{\vartheta}_i = \omega_{ms_i}^s \\ \dot{\omega}_{ms_i}^s = -\beta_i^2 \vartheta_i - 2\beta_i \omega_{ms_i}^s + \eta_i, \end{cases} \quad i = x, y, z \quad (15)$$

where  $\vartheta = [\vartheta_x \ \vartheta_y \ \vartheta_z]^T$  is the flexure angle,  $\eta = [\eta_x \ \eta_y \ \eta_z]^T$  is Gaussian white noise with the variance  $\sigma_\eta = [\sigma_{\eta_x} \ \sigma_{\eta_y} \ \sigma_{\eta_z}]^T$ ,  $\beta = [\beta_x \ \beta_y \ \beta_z]^T$  is the model parameter correlated to correlation time  $\tau_i$  satisfies:

$$\beta_i = 2.146/\tau_i, \quad (i = x, y, z) \quad (16)$$

From Equation (12) and (13), it can be easily observed that the measured projection of M-INS and S-INS in inertial frame can used as a matching scheme for transfer alignment. In this respect, the next section is devoted to constructing a unified linear transfer alignment model with vector observations.

### III. A UNIFIED NONSINGULAR RAPID LINEAR TRANSFER ALIGNMENT MODEL

In this section we will build a unified linear transfer alignment model with inherent biases in inertial sensors and flexible.

It is noticed that disturbed terms in equation (12) and (13), random noise, residue term of lever arm effects and the flexure angle rate, which corrupt the specific force and rate measurements will be attenuated due to the smoothing characteristic of integration process. The reduced measurement noise should improve filter performance in the estimation of misalignment angle.

The integration of the left-hand side of equation (12) over the time interval of interest is given below

$$\begin{cases} \hat{V}_S^{i_s} = \int_0^t \hat{f}_S^{i_s}(\tau) d\tau = \int_0^t \hat{C}_S^{i_s}(\tau) \hat{f}_S^{i_s}(\tau) d\tau \\ \delta \hat{V}_S^{i_s} = \int_0^t (\hat{f}_S^{i_s} \times \phi_S^{i_s} + \hat{C}_S^{i_s} \nabla^s + \hat{C}_S^{i_s} w_a^s) d\tau \end{cases} \quad (17)$$

Integrating the right-hand side of Equation (12) yields

$$\begin{cases} \hat{V}_m^{i_m} = \int_0^t \hat{f}_{mc}^{i_m}(\tau) d\tau = \int_0^t C_m^{i_m}(\tau) \hat{f}_{mc}^m(\tau) d\tau \\ \hat{w}_f^{i_m} = - \int_0^t C_m^{i_m}(\tau) w_f^m d\tau \end{cases} \quad (18)$$

Substituting equation (17) and (18) into equation (12) gives

$$\hat{V}_s^{i_s} - \delta V_s^{i_s} = C_{i_m}^{i_s} (\hat{V}_m^{i_m} + \bar{w}_f^{i_m}) \quad (19)$$

In the same way that equation (19) was obtained, integrating equation (13) on both sides over the time interval of interest, we have

$$\hat{\Omega}_s^{i_s} - \delta \Omega_s^{i_s} = C_{i_m}^{i_s} (\Omega_m^{i_m} + \bar{w}_\omega^{i_m}) \quad (20)$$

in which

$$\begin{cases} \Omega_S^{i_s} = \int_0^t \hat{\omega}_{i_s}^{i_s}(\tau) d\tau = \int_0^t \hat{C}_S^{i_s}(\tau) \hat{\omega}_{i_s}^{i_s}(\tau) d\tau \\ \delta \Omega_S^{i_s} = \int_0^t (\hat{\omega}_{i_s}^{i_s} \times \phi_S^{i_s} + \hat{C}_S^{i_s} \epsilon^S + \hat{C}_S^{i_s} \omega_{ms}^S) d\tau \end{cases} \quad (21)$$

and

$$\begin{cases} \Omega_m^{i_m} = \int_0^t \hat{\omega}_{i_m}^{i_m}(\tau) d\tau = \int_0^t \hat{C}_m^{i_m}(\tau) \hat{\omega}_{i_m}^{i_m}(\tau) d\tau \\ \bar{w}_\omega^{i_m} = \int_0^t C_m^{i_m}(\tau) w_{ms}^m(\tau) d\tau = \int_0^t C_m^{i_m}(\tau) C_s^m(\tau) w_{ms}^s(\tau) d\tau \end{cases} \quad (22)$$

where the  $w_{ms}^s$  is residue term of flexure effects.

Note that we found the equation (19) and (20) are derived without any assumption on misalignment. In other words, the integration matching formula can be written in the same form whether the misalignment angle is small or not. In this way, a unified rapid transfer alignment can be designed in inertial frame based on equation (19) and (20). Next, a unified nonsingular rapid transfer alignment solution is proposed based on integration of specific force and angular rate matching scheme. In alignment process, the M-INS is required to output the angular rate and specific force at each sampling period in the alignment process, and moreover, the precise attitude at the end of the alignment.

### A. UNIFIED ALIGNMENT MODEL BASED ON ATTITUDE MATRIX

For the S-INS, the initial alignment is a process that determination a coordinate transformation matrix from the body frame to the navigation frame  $n$ , namely the attitude matrix  $C_s^n(t)$ , which can be decomposed into four parts at any time based on the chain rule of the attitude matrix as follows:

$$C_s^n(t) = C_m^n(t) C_{i_m}^m(t) C_{i_s}^{i_m} C_s^{i_s}(t) \quad (23)$$

where  $C_m^n(t)$  is attitude matrix of M-INS,  $C_{i_m}^m(t)$  and  $C_s^{i_s}(t)$  can be obtained from the results of equation (5) and (6) in previous subsection. Hereby, the main problem is the estimation of the attitude matrix  $C_{i_s}^{i_m}$ , the relative orientation of M-INS and S-INS, which is an unknown constant quantity. The continuous time  $C_s^n(t)$  could be obtained by equation (23), which forms the basis for transfer alignment.

Based on equation (17) and (18), we can design a matching scheme for rapid transfer alignment in form of attitude matrix representation, which transforms the attitude-alignment problem into a continuous estimation of the relative attitude between the M-INS and S-INS problem.

While neglecting the flexure of the S-INS,  $C_{i_m}^{i_s}$  can be considered as a constant attitude matrix during the alignment process. Therefore, the attitude matrix  $C_{i_m}^{i_s}$  satisfies the following the differential equation

$$\dot{C}_{i_m}^{i_s} = \mathbf{0}_{3 \times 3} \quad (24)$$

Equations (7), (15), (17), (21), and (24) constitute the dynamic error model or the system equations. Taking the gyroscope drifts  $\epsilon^S$  and accelerometer biases  $\nabla^S$  into account as constant, the complete matrix state variable in the transfer alignment algorithm is selected as follows

$$X = \begin{bmatrix} C_{i_m}^{i_s} & \delta V_s^{i_s} & \delta \Omega_s^{i_s} & \phi_s^{i_b} & \epsilon^S & \nabla^S & \vartheta & \omega_{ms}^S \end{bmatrix} \quad (25)$$

We have added the  $\delta V_s^{i_s}$  and  $\delta \Omega_s^{i_s}$  into states for convenience of the numerical integrations computation, because it would be difficult to finish numerical integrations accurately from other coupled sub-states. With such state augmentation, the integrations process can effectively take advantage of the Kalman filter time-update equation and avoids numerical integrations problems.

Assume that the bias gyroscope drifts  $\epsilon^S$  and accelerometer biases  $\nabla^S$  are time invariant, i.e.,

$$\epsilon_{k+1}^S = \epsilon_k^S \quad (26)$$

$$\nabla_{k+1}^S = \nabla_k^S \quad (27)$$

where  $w_{gk}, w_{ak}$  are zero-mean white Gaussian noise sequence.

Combining Equations (7), (15), (17), (21), (24), (26) and (27) together, we obtain the dynamics model governed by the difference equation

$$X_{k+1} = \sum_{r=1}^7 \Phi_k^r X_k \Theta_k^r + W_k \quad (28)$$

The dynamics matrices,  $\Phi_k^r, \Theta_k^r$  in Equation (28) are defined as

$$\begin{aligned} \Phi_k^1 &= I_3 & \Theta_k^1 &= I_{10} \\ \Phi_k^2 &= [\hat{f}_s^{i_s} \times] & \Theta_k^2 &= E^{6,4} \Delta t \\ \Phi_k^3 &= \hat{C}_s^{i_s} & \Theta_k^3 &= E^{8,4} \Delta t + E^{7,5} \Delta t - E^{7,6} \Delta t + E^{10,5} \Delta t \\ \Phi_k^4 &= [\hat{\omega}_s^{i_s} \times] & \Theta_k^4 &= E^{6,5} \Delta t \\ \Phi_k^5 &= I_3 & \Theta_k^5 &= E^{10,9} \Delta t \\ \Phi_k^6 &= -\text{diag}[\beta_i^2 \times] & \Theta_k^6 &= E^{9,10} \Delta t \\ \Phi_k^7 &= -\text{diag}[2 \cdot \beta_i \times] & \Theta_k^7 &= E^{10,10} \Delta t \end{aligned} \quad (29)$$

where  $E^{i,j}$  denote a  $10 \times 10$  matrix with 1 in the element  $(ij)$  and 0 elsewhere.

### B. MEASUREMENT MODEL

The measurement model is

$$Z_{k+1} = \begin{bmatrix} \hat{V}_{s_k}^{i_s} & \hat{\Omega}_{s_k}^{i_s} \end{bmatrix} = H_{k+1}^m X_{k+1} G_{k+1}^m + V_{k+1} \quad (30)$$

where the observation matrices are

$$\mathbf{H}_{k+1}^m = \mathbf{I}_3, \quad \mathbf{G}_{k+1}^m = \begin{bmatrix} \mathbf{V}_{m_k}^{i_m} & \mathbf{\Omega}_{m_k}^{i_m} \\ 1 & 0 \\ 0 & 1 \\ \mathbf{0}_{5 \times 1} & \mathbf{0}_{5 \times 1} \end{bmatrix} \quad (31)$$

and the measurement noise covariance matrix is

$$\mathbf{R}_{k+1} = \begin{bmatrix} \sigma_v^2 \mathbf{I}_3 & \mathbf{0}_{3 \times 3} \\ \mathbf{0}_{3 \times 3} & \sigma_\omega^2 \mathbf{I}_3 \end{bmatrix} \quad (32)$$

### C. STATE-MATRIX KALMAN FILTER UPDATE

Due to the existence of matrix in filter state, the filter update equations are not the same with the traditional vector Kalman filter, They can be summarize as follows, and readers can refer to [34] for more analysis and additional derivations.

1) Time update equations

$$\mathbf{X}_{k+1} = \sum_{r=1}^7 \mathbf{\Phi}_k^r \mathbf{X}_{k+1} \mathbf{\Theta}_k^r + \mathbf{W}_k \quad (33)$$

$$\mathbf{\Psi}_k = \sum_{r=1}^7 \left[ (\mathbf{\Theta}_k^r)^T \otimes \mathbf{\Phi}_k^r \right] \quad (34)$$

$$\mathbf{P}_{k+1/k} = \mathbf{\Psi}_k \mathbf{P}_{k/k} \mathbf{\Psi}_k^T + \mathbf{Q}_k \quad (35)$$

2) Measurement update equations

$$\tilde{\mathbf{Z}}_{k+1} = \mathbf{Z}_{k+1} - \mathbf{H}_{k+1}^m \hat{\mathbf{X}}_{k+1/k} \mathbf{G}_{k+1}^m \quad (36)$$

$$\mathbf{\Gamma}_{k+1} = (\mathbf{G}_{k+1}^m)^T \otimes \mathbf{H}_{k+1}^m \quad (37)$$

$$\mathbf{S}_{k+1} = \mathbf{\Gamma}_{k+1} \mathbf{P}_{k+1/k} (\mathbf{\Gamma}_{k+1})^T + \mathbf{R}_{k+1} \quad (38)$$

$$\mathbf{K}_{k+1} = \mathbf{P}_{k+1/k} (\mathbf{\Gamma}_{k+1})^T (\mathbf{S}_{k+1})^{-1} \quad (39)$$

$$\hat{\mathbf{X}}_{k+1/k+1} = \hat{\mathbf{X}}_{k+1/k} + \sum_{j=1}^{10} \sum_{i=1}^2 \mathbf{K}_{k+1}^{j,i} \tilde{\mathbf{Y}}_{k+1} \mathbf{\Xi}^{ij} \quad (40)$$

$$\mathbf{P}_{k+1/k+1} = (\mathbf{I}_{30} - \mathbf{K}_{k+1} \mathbf{\Gamma}_{k+1}) \mathbf{P}_{k+1/k} (\mathbf{I}_{30} - \mathbf{K}_{k+1} \mathbf{\Gamma}_{k+1})^T + \mathbf{K}_{k+1} \mathbf{R}_{k+1} \mathbf{K}_{k+1}^T \quad (41)$$

where  $\otimes$  denotes the Kronecker product [34],  $\mathbf{K}_{k+1}^{j,i}$  is a  $3 \times 3$  submatrix of the  $30 \times 6$  matrix  $\mathbf{K}_{k+1}$  defined by

$$\mathbf{K}_{k+1} \begin{bmatrix} \mathbf{K}_{k+1}^{1,1} & \mathbf{K}_{k+1}^{1,2} \\ \vdots & \vdots \\ \mathbf{K}_{k+1}^{10,1} & \mathbf{K}_{k+1}^{10,2} \end{bmatrix} \quad (42)$$

and where  $\mathbf{\Xi}^{ij}$  denote a  $2 \times 10$  matrix with 1 in the element  $(ij)$  and 0 elsewhere.

It is well known that attitude matrix is an orthogonal matrix as it is a rotation matrix. Therefore, a good estimate of state is one that is nearly orthogonal. Hence we use a simple and popular orthogonalization solution called ‘‘Optimal Brute-Force (OBF)’’ orthogonalization [36]. In this method, once Kalman filter has computed the a posteriori estimate,  $\hat{\mathbf{C}}_{i_m}^{i_s}$ , the optimization problem, known as the orthogonal Procrustes problem, has the following closed form solution

$$\bar{\mathbf{C}}_{i_m}^{i_s} = \hat{\mathbf{C}}_{i_m}^{i_s} \left( \hat{\mathbf{C}}_{i_m}^{i_s T} \hat{\mathbf{C}}_{i_m}^{i_s} \right)^{-\frac{1}{2}} \quad (43)$$

The orthogonal estimate,  $\bar{\mathbf{C}}_{i_m}^{i_s}$ , is then substituted for  $\hat{\mathbf{C}}_{i_m}^{i_s}$  in the next propagation process. This technique is called ‘‘Brute-Force’’ orthogonalization because the orthogonalization procedure is performed outside the filter.

## IV. MONTE CARLO SIMULATION RESULTS AND DISCUSSION

In order to assess the performance of rapid transfer alignment scheme based on matrix Kalman filter (MKFTA), a Monte-Carlo simulation has been performed in this section. We describe the results from 100-sample Monte Carlo cases represented by the sway maneuver under both the small and large misalignment angle cases. In the first case, the precision and speed performances of the proposed algorithm are compared with traditional rapid transfer alignment algorithm referred to RAP (Rapid Alignment Prototype) with VAM [2]. However, the RAP is valid only for the case where attitude errors are small enough, called the small misalignment model (SMM) here. And this condition is a limitation in applying the RAP in certain domains. In the second case, we apply UKF as in [19] to the transfer alignment with velocity and calculated misalignment angle matching based on nonlinear model called as the large misalignment model (LMM).

### A. SIMULATION CONDITION

To simulate the local vibration by S-INS side, the flexure misalignment angle is modeled as a second order Markov process in equation (15):

Denote the variance of the flexure angle  $\sigma_\vartheta = [\sigma_{\vartheta_x} \ \sigma_{\vartheta_y} \ \sigma_{\vartheta_z}]^T$ .  $\sigma_\eta$ ,  $\sigma_\vartheta$ ,  $\beta$  and  $\tau$  have the following relation:

$$\sigma_{\eta_i} = (4\beta_i^3 \sigma_{\vartheta_i})^2, \quad \beta_i = \frac{2.146}{\tau_i} \quad (44)$$

In the simulations, we set  $\sigma_\vartheta = [(0.01^\circ)^2 \ (0.015^\circ)^2 \ (0.01^\circ)^2]^T$ ,  $\tau = [2 \ 1 \ 2]^T (s)$ .

Assuming that the precision of M-INS is much higher than that of S-INS, we can ignore the error of M-INS. The main specifications of the sensors of S-INS are shown in table 1. The sample rates of S-INS and M-INS are both 100Hz. The update rates of the filters are 50 Hz.

TABLE 1. Sensor specifications of the S-INS.

Parameters	Gyro	Accelerometer
Bias stability	10deg/h	1mg
Random walk	1deg/ $\sqrt{h}$	100ug $\cdot\sqrt{s}$

The misalignment condition is shown in table 2.

The wind wave will cause pitch, roll, surge, sway and heave of the carrier. The generalized straight and sway motion can

TABLE 2. Misalignment of the S-INS.

misalignment	Pitch	Roll	Heading
Small	1°	1°	1°
Large	60°	60°	150°

be described according to [19]:

$$\begin{cases} \theta = \theta_m \sin(\omega_\theta + \varphi_\theta) \\ \gamma = \gamma_m \sin(\omega_\gamma + \varphi_\gamma) \\ \psi = \psi_m \sin(\omega_\psi + \varphi_\psi) \end{cases} \quad (45)$$

where  $\theta, \gamma, \psi$  are the pitch, roll and heading, respectively;  $\theta_m, \gamma_m, \psi_m$  are the sway magnitudes;  $\omega_\theta, \omega_\gamma, \omega_\psi$  are the sway frequencies;  $\varphi_\theta, \varphi_\gamma, \varphi_\psi$  are the initial phases of the motion. These parameters are listed in table 3.

TABLE 3. Simulation parameters setting.

	Pitch	Roll	Heading
Swaying amplitude value	5°	3°	2°
Sway frequency	$2\pi * 0.5$	$2\pi * 0.3$	$2\pi * 0.4$
Initial phrase angle	0	0	0

In the simulation, the initial state covariance matrix is set as follows, and the more analysis and additional derivations can be found in [34].

$$\begin{cases} P_0 = \bar{P}_0 \otimes I_3 \\ \bar{P}_0 = \text{diag}([P_C, P_{\delta V}, P_{\delta \Omega}, P_\varphi, P_\varepsilon, P_\nabla, P_\vartheta, P_\omega]) \end{cases} \quad (46)$$

where  $P_{C_i} = (1)², P_{\delta V_i} = (1e - 4m/s)², P_{\delta \Omega_i} = (1e - 4°)², P_{\varphi_i} = (1e - 4')², P_{\varepsilon_i} = (10°/h)², P_{\nabla_i} = (1mg)², P_{\vartheta_i} = (1°)², P_{\omega_i} = (1°/s)²$ .

**B. SIMULATION RESULTS UNDER THE SWAY MANEUVER**

The transfer alignment progresses are calculated using traditional state vector KF and MKF, respectively. 10 seconds swing data is used for rapid transfer alignment to validate the proposed method. The results are illustrated in Figures 1-4 and table 4, correspondingly.

The mean values of misalignment estimate error at each time step for the proposed scheme and traditional scheme are depicted in figures 1 and 3, as well as their respective  $\pm 3\sigma$  envelopes. As expected, the MC-mean almost coincides with 0 in the steady-state, which clearly shows the unbiasedness of the MKF.

The  $\pm 3\sigma$  envelope of proposed method are clearly narrower and stabilizing time than that of the traditional method. In order to compare the performance further, the RMS estimation error is compared in figures 2 and 4. A similar comparison was done in [10] and [19], where we can see

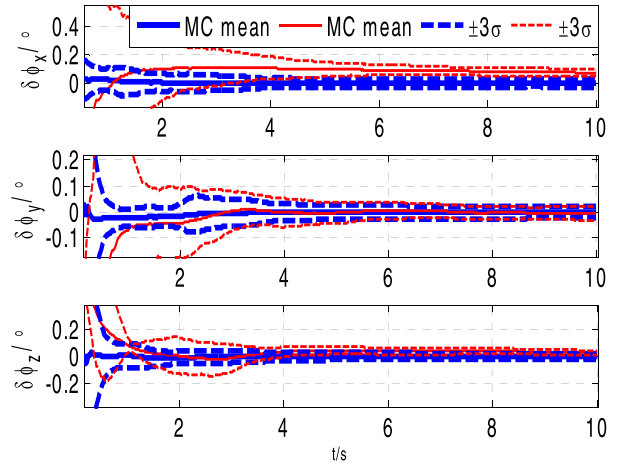


FIGURE 1. Monte-Carlo means and  $\pm 3\sigma$  envelopes of alignment angle estimation errors for SMM with the sway maneuver (proposed method: blue thick lines; traditional method: red thin lines; dashed lines are for  $3\sigma$  envelopes).

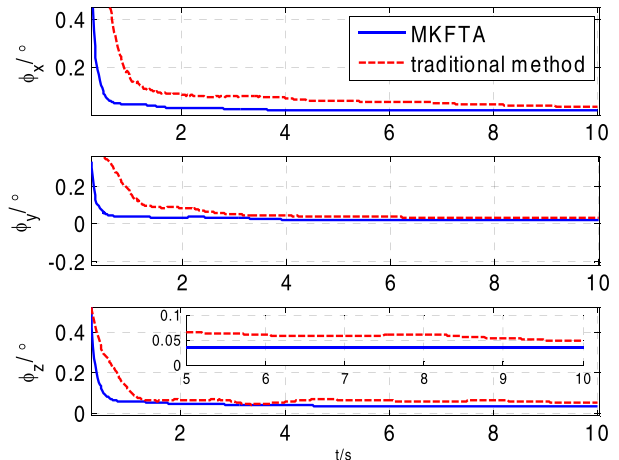
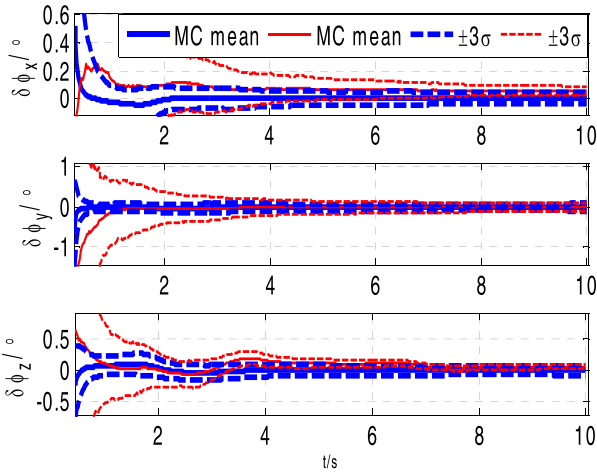


FIGURE 2. Misalignment estimation error RMS of SMM with the sway maneuver.

that the proposed scheme provides better RMS error performance than traditional method. Furthermore, figure 4 gives the results of our previous work [1]. It is known that the Rodrigues parameters have three parameters, as opposed to the six redundant elements of the attitude matrix. Accordingly, the estimation results of horizontal misalignment angles are slightly faster than MKFTA. It can be seen that the performances of the MKFTA and EKF2 are virtually identical due to the same matching scheme.

In order to examine the flexure effect, the RMS estimation error of misalignments for SMM and LMM, with and without the flexure compensation, are presented in Figures 5 and 6, respectively. The presence of the flexure effect leads to obvious degrade performance for misalignments estimation. When without not considering the flexure effect, the estimator provides the worst results; namely, it has the slower transient and the higher steady-state.



**FIGURE 3.** Monte-Carlo means and  $\pm 3\sigma$  envelopes of alignment angle estimation errors for LMM with the Sway Maneuver (proposed method: blue thick lines; traditional method: red thin lines; dashed lines are for  $3\sigma$  envelopes).

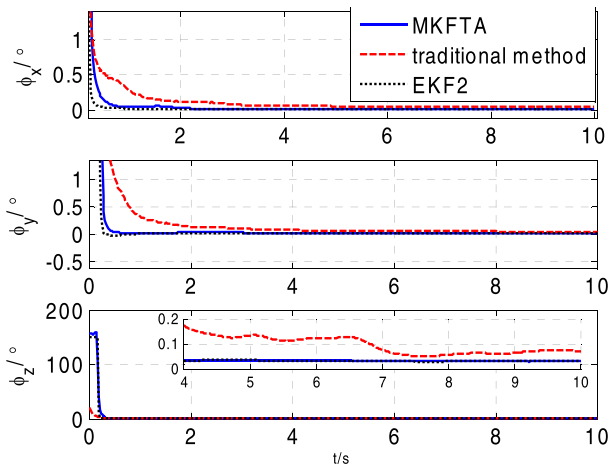


**FIGURE 4.** Misalignment estimation error RMS of LMM with the sway maneuver.

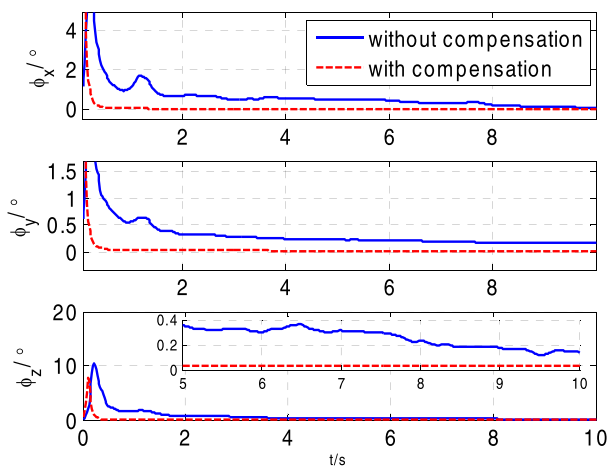


**FIGURE 5.** Misalignment estimation error RMS for SMM with and without the flexure effect compensation.

Figures 7 and 8 show that the MKF does a nice job of estimating the flexure. A rigorous global observability analysis theory [37], can explain why that the flexure angle is less

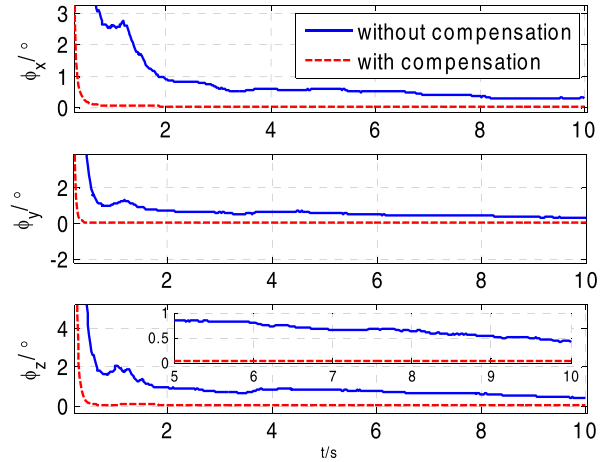


**FIGURE 6.** Misalignment estimation error RMS for LMM with and without the flexure effect compensation.

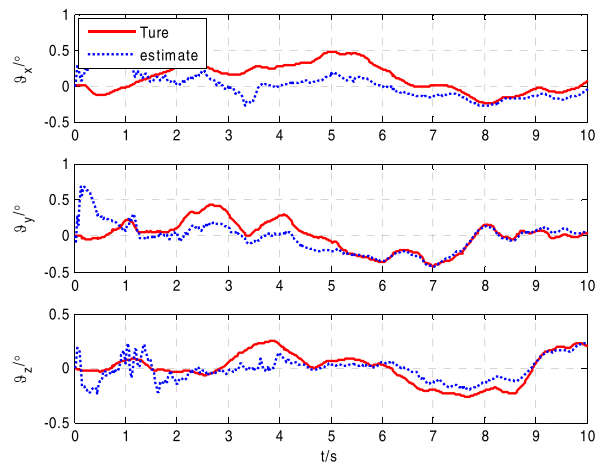


**FIGURE 7.** Estimate of the flexure angle.

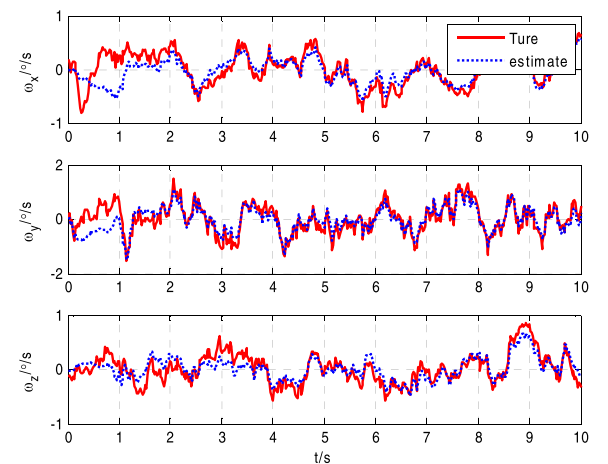


**FIGURE 8.** Estimate of the flexure angle rate.

observable than the flexure angle rate. The proposed alignment method takes into account the flexure effect ensuring convergence rate and sufficient accuracy of misalignments estimation in both SMM and LMM.

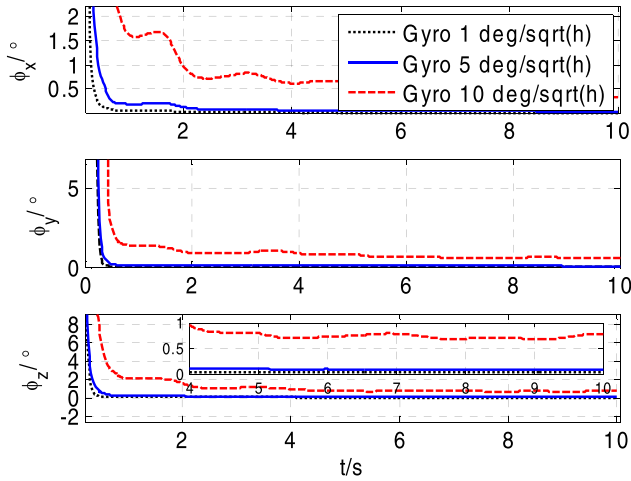


FIGURE 9. Misalignment estimation error RMS for LMM with different gyro random walk.

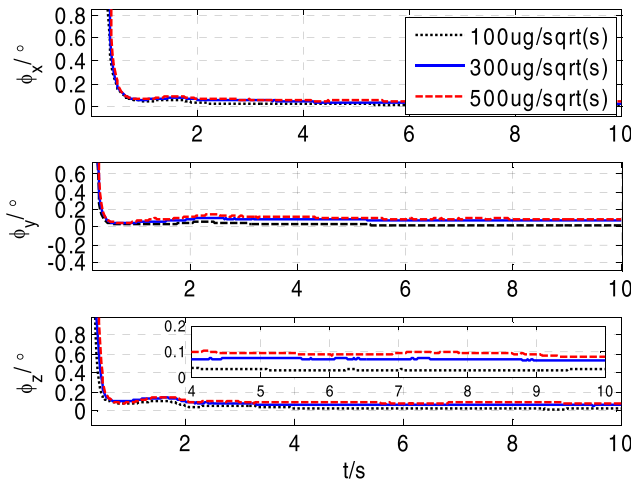


FIGURE 10. Misalignment estimation error RMS for LMM with different accelerometer noise.

It is well known that S-INS suffers from the mechanical vibrations in operational environment and the specification is generally worse than laboratory conditions [38]. One remaining question is, how does the MKFTA algorithm perform under practice vibrations conditions, especially when applied to outer missiles on the flexible wing? In order to analyze the influence of the inertial sensors noise on the performance of transfer alignment, different levels of inertial sensor noise are taken into account, adopting the scheme in [38]. The RMS errors of misalignment estimation are presented in Figures 9 and 10.

The figures show that the increased gyroscopes and accelerometers noise results in a decreased alignment performance and accuracy. Therefore, the sensor noise characteristics, which can vary with mechanical vibration, should be taken into account in the real system design and analysis. For best results, laboratory tests of the IMU under representative dynamics and vibration may also be conducted where suitable equipment is available.

As shown in figure 1-4, compared with the traditional scheme, the accuracy is significantly higher. The numerical

TABLE 4. Monte-Carlo means and RMS of the misalignment under the Sway Maneuver at the final time.

Misalignment	Scheme	Monte-Carlo simulations	$\phi_x$	$\phi_y$	$\phi_z$
[1° 1° 1°]	Traditional KF (linear model)	Mean	1.074	0.984	0.961
		RMS	0.036	0.036	0.049
	MKFTA(proposed unified model)	Mean	1.005	0.989	0.989
		RMS	0.021	0.020	0.033
[60° 60° 150°]	Traditional UKF(nonlinear model)	Mean	60.056	59.965	149.958
		RMS	0.049	0.055	0.069
	EKF2	Mean	60.020	59.982	149.985
		RMS	0.015	0.026	0.031
	MKFTA(proposed unified model)	Mean	59.990	59.984	149.986
		RMS	0.014	0.022	0.030

comparison of misalignment estimation results at the final time under the misalignment listed in table 2 is summarized in Table 4. Clearly, as expected, we can see that the proposed scheme outperforms the traditional scheme. The mean estimates of misalignments are  $[1.005^\circ \ 0.989^\circ \ 0.989^\circ]^T$  and  $[59.990^\circ \ 59.984^\circ \ 149.986^\circ]^T$  for the proposed MKFTA scheme, whereas  $[1.074^\circ \ 0.984^\circ \ 0.961^\circ]^T$  and  $[60.056^\circ \ 59.965^\circ \ 149.958^\circ]^T$  for the traditional scheme. RMS estimation errors of the proposed MKFTA scheme are  $[0.021^\circ \ 0.020^\circ \ 0.033^\circ]^T$  and  $[0.014^\circ \ 0.022^\circ \ 0.030^\circ]^T$  at 10s, in contrast with the traditional methods  $[0.036^\circ \ 0.036^\circ \ 0.049^\circ]^T$  and  $[0.049^\circ \ 0.055^\circ \ 0.069^\circ]^T$ .

C. DISCUSSION

In this section, an extensive Monte Carlo simulation was performed in order to evaluate the availability of the proposed algorithm. Compared with the conventional method, it is apparent that the proposed scheme performs better not only at the beginning of the estimate, but also in steady state. For the proposed transfer alignment scheme, we have held the following statements.

- We proposed a unified nonsingular model, without the need to know the relative orientation relationship of M-INS and S-INS, and there is no singularity problem at any orientation of the rigid body, since we derived the alignment model in form of attitude matrix without making any assumption on the misalignment angle.
- The estimation performance of proposed scheme is better: the transition phases are shorter and the steady-state errors are smaller. The Monte-Carlo means and standard deviations of all the misalignment estimation error in the proposed scheme are much more damped. Thus, the proposed scheme meets the rapidity and accuracy requirements for tactical weapon transfer alignment at the same time.
- The derivation of the MKF shows that it is a direct generalization of the classical vector Kalman filter. The computation cost of proposed linear MKF based alignment scheme is similar to that of the standard linear KF,

which means that the proposed scheme has lower the filter computational burden than traditional UKF.

Besides aforementioned characteristics, no prior information of the initialization values is needed for proposed scheme, whereas, the traditional method needs the process with a ‘one-shot’ transfer of data from the M-INS. On the other hand, by taking the flexure angle and rate as estimate items, the proposed method improves the transfer alignment accuracy.

## V. CONCLUSION

The rapid and accurate transfer alignment is vitally important for S-INS, which influences the performance of S-INS largely. Based on attitude matrix representation, this paper proposes a unified model under arbitrary misalignment angles for transfer alignment based on integral of specific force and rate matching, which is derived from the traditional acceleration and rate matching. Furthermore, we implement MKF for this plant. The update process is similar to the standard linear KF, and the computational savings can be significant in contrast to the traditional nonlinear filter. As a result, the state estimate would be as straightforward as that of the attitude matrix, and not need to be extracted by some numerical method [5]–[7].

Monte-Carlo simulations with sway maneuvers under both small and large misalignment angle cases are conducted to evaluate the proposed transfer alignment algorithm. Simulation results demonstrate that the proposed transfer alignment scheme can be accomplished within ten seconds, and even less than 1 mrad accuracy can be achieved whether the initial misalignment is small or large. Furthermore, the proposed scheme presents greatly improved performance (compared with the traditional KF for linear model in accuracy and UKF for nonlinear model scheme in the computation cost).

## ACKNOWLEDGMENT

The authors also would thank Yang Liu of Northwestern Polytechnical University for helping edit the language of the paper.

## REFERENCES

- X. Cui, C. Mei, Y. Qin, G. Yan, and Z. Liu, “A unified model for transfer alignment at random misalignment angles based on second-order EKF,” *Meas. Sci. Technol.*, vol. 28, no. 4, pp. 1–10, Feb. 2017, doi: [10.1088/1361-6501/aa5b75](https://doi.org/10.1088/1361-6501/aa5b75).
- J. Kain and J. Cloutier, “Rapid transfer alignment for tactical weapon applications,” in *Proc. AIAA Guid., Navigat. Control Conf.*, Boston, MA, USA, 1989, p. 3581.
- D. Choukroun, I. Y. Bar-Itzhack, and Y. Oshman, “Optimal-REQUEST algorithm for attitude determination,” *J. Guid., Control, Dyn.*, vol. 27, no. 3, pp. 418–425, May 2004, doi: [10.2514/1.10337](https://doi.org/10.2514/1.10337).
- M. D. Shuster and S. D. Oh, “Three-axis attitude determination from vector observations,” *J. Guid. Control, Dyn.*, vol. 4, no. 1, pp. 70–77, 1981, doi: [10.2514/3.19717](https://doi.org/10.2514/3.19717).
- Y. X. Wu and X. F. Pan, “Velocity/position integration formula Part I: Application to in-flight coarse alignment,” *IEEE Trans. Aerosp. Electron. Syst.*, vol. 49, no. 2, pp. 1006–1023, Apr. 2013, doi: [10.1109/TAES.2013.6494395](https://doi.org/10.1109/TAES.2013.6494395).
- L. Chang, J. Li, and S. Chen, “Initial alignment by attitude estimation for strapdown inertial navigation systems,” *IEEE Trans. Instrum. Meas.*, vol. 64, no. 3, pp. 784–794, Mar. 2015, doi: [10.1109/TIM.2014.2355652](https://doi.org/10.1109/TIM.2014.2355652).
- L. Chang, B. Hu, and Y. Li, “Backtracking integration for fast attitude determination-based initial alignment,” *IEEE Trans. Instrum. Meas.*, vol. 64, no. 3, pp. 795–803, Mar. 2015, doi: [10.1109/TIM.2014.2359516](https://doi.org/10.1109/TIM.2014.2359516).
- J. Li, J. Xu, L. Chang, and F. Zha, “An improved optimal method for initial alignment,” *J. Navigat.*, vol. 67, no. 4, pp. 727–736, Jul. 2014, doi: [10.1017/S0373463314000198](https://doi.org/10.1017/S0373463314000198).
- L. Xie and J. Lu, “Optimisation-based transfer alignment and calibration method for inertial measurement vector integration matching,” *J. Navigat.*, vol. 70, no. 3, pp. 595–606, May 2017, doi: [10.1017/S0373463316000680](https://doi.org/10.1017/S0373463316000680).
- J. Lu, L. Xie, and B. Li, “Applied quaternion optimization method in transfer alignment for airborne AHRS under large misalignment angle,” *IEEE Trans. Instrum. Meas.*, vol. 65, no. 2, pp. 346–354, Feb. 2016, doi: [10.1109/TIM.2015.2502838](https://doi.org/10.1109/TIM.2015.2502838).
- P. D. Groves, “Optimising the transfer alignment of weapon INS,” *J. Navigat.*, vol. 56, no. 2, pp. 323–335, May 2003, doi: [10.1017/S0373463303002261](https://doi.org/10.1017/S0373463303002261).
- D. Yang, S. Wang, H. Li, Z. Liu, and J. Zhang, “Performance enhancement of large-ship transfer alignment: A moving horizon approach,” *J. Navigat.*, vol. 66, no. 1, pp. 17–33, Jan. 2013, doi: [10.1017/S037346331200032X](https://doi.org/10.1017/S037346331200032X).
- M. C. Havinga, “Flight test results of a MEMS IMU based transfer alignment algorithm for short range air-to-air missiles,” in *Proc. AIAA Guid., Navigat., Control Conf.*, Boston, MA, USA, 2013, pp. 5244–5346.
- J. Wendel, J. Metzger, and G. Trommer, “Rapid transfer alignment in the presence of time correlated measurement and system noise,” in *Proc. AIAA Guid., Navigat., Control Conf. Exhibit*, Providence, RI, USA, 2004, pp. 1–12.
- R. Rogers, “Velocity-plus-rate matching for improved tactical weapon rapid transfer alignment,” in *Proc. Navigat. Control Conf.*, New Orleans, LA, USA, 1991, p. 2783.
- X. Cui, C. Mei, Y. Qin, G. Yan, and Q. Fu, “In-motion alignment for low-cost SINS/GPS under random misalignment angles,” *J. Navigat.*, vol. 70, no. 6, pp. 1224–1240, Nov. 2017, doi: [10.1017/S037346331700039X](https://doi.org/10.1017/S037346331700039X).
- D. Zhou and L. Guo, “Stochastic integration H $\infty$  filter for rapid transfer alignment of INS,” *Sensors*, vol. 17, no. 11, p. 2670, Nov. 2017, doi: [10.3390/s17112670](https://doi.org/10.3390/s17112670).
- H. Chu, T. Sun, B. Zhang, H. Zhang, and Y. Chen, “Rapid transfer alignment of MEMS SINS based on adaptive incremental Kalman filter,” *Sensors*, vol. 17, no. 1, p. 152, Jan. 2017, doi: [10.3390/s17010152](https://doi.org/10.3390/s17010152).
- Y. Hao, Z. Xiong, W. Wang, and F. Sun, “Rapid transfer alignment based on unscented Kalman filter,” in *Proc. Amer. Control Conf.*, Minneapolis, MN, USA, 2006, pp. 2215–2220.
- E.-H. Shin and N. El-Sheimy, “An unscented Kalman filter for in-motion alignment of low-cost IMUs,” in *Proc. PLANS Position Location Navigat. Symp.*, Monterey, CA, USA, 2004, pp. 273–279.
- W. Zhanqing, L. Lihua, L. Xin, and Z. Yanshun, “Transfer alignment of shipborne aircraft with large misalignment based on rotation vector error model,” *J. Chin. Inertial Technol.*, vol. 24, no. 6, pp. 723–729, Dec. 2016.
- J. Cheng, T. Wang, L. Wang, and Z. Wang, “A new polar transfer alignment algorithm with the aid of a star sensor and based on an adaptive unscented Kalman filter,” *Sensors*, vol. 17, no. 10, p. 2417, Oct. 2017, doi: [10.3390/s17102417](https://doi.org/10.3390/s17102417).
- Y. Wang, F. Sun, Y. Zhang, H. Liu, and H. Min, “Central difference particle filter applied to transfer alignment for SINS on missiles,” *IEEE Trans. Aerosp. Electron. Syst.*, vol. 48, no. 1, pp. 375–387, Jan. 2012, doi: [10.1109/TAES.2012.6129642](https://doi.org/10.1109/TAES.2012.6129642).
- S. Chattaraj and A. Mukherjee, “Particle filter based attitude matching algorithm for in-flight transfer alignment,” in *Proc. 8th Int. Conf. Elect. Comput. Eng.*, Dhaka, Bangladesh, 2014, pp. 788–791.
- J. Sun, X.-S. Xu, Y.-T. Liu, T. Zhang, and Y. Li, “Initial alignment of large azimuth misalignment angles in SINS based on adaptive UPF,” *Sensors*, vol. 15, no. 9, pp. 21807–21823, Aug. 2015, doi: [10.3390/s150921807](https://doi.org/10.3390/s150921807).
- C. Y. Yu, N. El-Sheimy, H. Y. Lan, and Z. B. Liu, “Map-based indoor pedestrian navigation using an auxiliary particle filter,” *Micromachines*, vol. 8, no. 7, p. 225, Jul. 2017, doi: [10.3390/mi8070225](https://doi.org/10.3390/mi8070225).
- A. Masiero, A. Guarnieri, F. Pirotti, and A. Vettore, “A particle filter for smartphone-based indoor pedestrian navigation,” *Micromachines*, vol. 5, no. 4, pp. 1012–1033, Nov. 2014, doi: [10.3390/mi5041012](https://doi.org/10.3390/mi5041012).
- Q. Fu, Y. Liu, Z. Liu, S. Li, and B. Guan, “Autonomous in-motion alignment for land vehicle strapdown inertial navigation system without the aid of external sensors,” *J. Navigat.*, vol. 71, no. 6, pp. 1312–1328, Nov. 2018, doi: [10.1017/S0373463318000437](https://doi.org/10.1017/S0373463318000437).

- [29] Y. Lu and X. Cheng, "Random misalignment and lever arm vector online estimation in shipborne aircraft transfer alignment," *Measurement*, vol. 47, pp. 756–764, Jan. 2014, doi: [10.1016/j.measurement.2013.09.032](https://doi.org/10.1016/j.measurement.2013.09.032).
- [30] P. G. Savage, "Lever arm corrections during INS transfer alignment with wide angle initial heading error," Strapdown Associates, Maple Plain, MN, USA, Tech. Rep. SAI-WBN-14008, 2015. [Online]. Available: [www.strapdownassociates.com](http://www.strapdownassociates.com)
- [31] A. G. Pehlivanoglu and Y. Ercan, "Investigation of flexure effect on transfer alignment performance," *J. Navigat.*, vol. 66, no. 1, pp. 1–15, Jan. 2013, doi: [10.1017/S0373463312000306](https://doi.org/10.1017/S0373463312000306).
- [32] Z. Liu, Y. Qin, S. Li, and X. Cui, "A new IMU-based method for relative pose determination," in *Proc. 22nd Saint Petersburg Int. Conf. Integr. Navigat. Syst.*, Saint Petersburg, Russia, 2015, pp. 425–428.
- [33] R. E. Kalman, "A new approach to linear filtering and prediction problems," *J. Basic Eng.*, vol. 82, no. 1, pp. 35–45, Mar. 1960, doi: [10.1115/1.3662552](https://doi.org/10.1115/1.3662552).
- [34] D. Choukroun, H. Weiss, I. Y. Bar-Itzhack, and Y. Oshman, "Kalman filtering for matrix estimation," *IEEE Trans. Aerosp. Electron. Syst.*, vol. 42, no. 1, pp. 147–159, Jan. 2006, doi: [10.1109/TAES.2006.1603411](https://doi.org/10.1109/TAES.2006.1603411).
- [35] D. Mortari, F. L. Markley, and P. Singla, "Optimal linear attitude estimator," *J. Guid., Control, Dyn.*, vol. 30, no. 6, pp. 1619–1627, Nov. 2007, doi: [10.2514/1.29568](https://doi.org/10.2514/1.29568).
- [36] F. L. Markley and D. Mortari. (Nov. 1999). *How to Estimate Attitude from Vector Observation*. [Online]. Available: <http://www.researchgate.net/publication/252610346>
- [37] Y. Tang, Y. WU, M. Wu, W. Wu, X. Hu, and L. Shen, "INS/GPS integration: Global observability analysis," *IEEE Trans. Veh. Technol.*, vol. 58, no. 3, pp. 1129–1142, Mar. 2009, doi: [10.1109/TVT.2008.926213](https://doi.org/10.1109/TVT.2008.926213).
- [38] J. Wendel and G. F. Trommer, "IMU Performance requirement assessments for GPS/INS missile navigation systems," in *Proc. 58th Annu. Meeting Inst. Navigat. CIGTF 21st Guid. Test Symp.*, Albuquerque, NM, USA, 2002, pp. 82–88.



**XIAO CUI** received the M.S. degree in navigation, guidance and control from Northwestern Polytechnical University, Xi'an, China, in 2013, where he is currently pursuing the Ph.D. degree with the Department of Measurement and Control Technology and Instrument Engineering. He holds three patents. His research interests include precise air-drop systems and navigation systems.



**GONGMIN YAN** was born in 1977. He received the B.S. degree in automatic control and the Ph.D. degree in navigation, guidance and control from Northwestern Polytechnical University, in 2000 and 2006, respectively. He is currently an Associate Professor with the School of Automation, Northwestern Polytechnical University. He has authored more than 30 scientific publications including one book. His research interests include inertial navigation, integrated navigation, and data fusion.



**QIANGWEN FU** received the M.S. and Ph.D. degrees in precision instrument and machinery from the School of Automation, Northwestern Polytechnical University (NWPU), Xi'an, China, in 2005 and 2015, respectively. He is currently an Assistant Researcher with the School of Automation, NWPU, where he is also a member of the INS and Multi-sensor Integrated Navigation Research Group. His research interests include vehicle positioning and orientation system and multi-sensor integrated navigation. He is a member of the Chinese Society of Inertial Technology.



**QI ZHOU** received the B.S., M.S., and Ph.D. degrees in navigation, guidance and control from the School of Automation, Northwestern Polytechnical University, Xi'an, China, in 2007, 2008, and 2013, respectively. He is currently a Senior Engineer with the Science and Technology on Aircraft Control Laboratory, Xi'an Flight Automatic Control Research Institute. His research interests include polar inertial navigation and multi-sensor integrated navigation.



**ZHENBO LIU** received the B.S. and M.S. degrees in precision instrument and machinery from the School of Automation, Northwestern Polytechnical University (NWPU), Xi'an, China, in 2011 and 2014, respectively. He is currently pursuing the Ph.D. degree with the School of Automation, NWPU, and with the Department of Geomatics Engineering, University of Calgary. His current research interest focuses on low-cost IMU-based navigation integrated with aiding sensors, such as odometer, camera, or LiDAR for unmanned ground vehicle in GNSS denied environment. He is a Student Member of the Institute of Navigation and the Chinese Society of Inertial Technology.

...